MRS Advances
https://doi.org/10.1557/s43580-023-00556-8

ORIGINAL PAPER

Engineering highly fluorescent and colloidally stable $CsPbBr_3$ nanocrystals of different shapes using imidazolium-based polysalt ligands

Unaisah Vorajee[1] · Selin Donmez[1] · Sisi Wang[1] · Hedi Mattoussi[1]

Received: 11 January 2023 / Accepted: 22 March 2023

Abstract
We applied a multidentate imidazolium bromide polymer coating to $CsPbBr_3$ perovskite nanocrystals and nanoplatelets to provide passivation of surface vacancies and preservation of the nanocrystal integrity. This ligand is complexed with an additional bromide-based salt, $PbBr_2$ or $CoBr_2$, to overcome the largely damaging effects of etching while imparting colloidal and morphological stability. Photoluminescence quantum yield measurements yielded near-unity for nanocubes and ~ 70 to 80% for nanoplatelets. Structural characterizations showed that application of the ligand or ligand-salt complex does not alter the crystal structure or morphology of the nanocrystals.

Introduction

Colloidal lead halide perovskite nanocrystals have recently gained much interest due to their unique optoelectronic properties. These include tunable and narrow photoluminescence (PL) profiles, high PL quantum yields (PLQY), along with relatively easy to implement synthesis [1, 2]. These attractive qualities make them a great candidate for potential use in several applications, such as lasers, solar cells, photodetectors, and light-emitting diodes (LEDs) [1, 3–5]. One major problem encountered by these materials has been their colloidal and structural instability. This problem has been attributed to the ionic nature of the core combined with the highly dynamic binding exhibited by the native molecular scale ligands used during growth of the nanocrystals, namely oleylamine (OLA) and oleic acid (OA) [6, 7]. As a result, deterioration of the as-prepared materials takes place and progressively shifts the surface stoichiometry from anion-rich to lead-rich [7]. This creates vacancies that act as trap states for charge carriers, which increases the nonradiative recombination rates and lowers the overall PLQY [8].

One strategy that has been tested by a few groups for repairing the surface defects in $CsPbBr_3$ nanocrystals has relied on the use of electrostatic interactions between bromide-based salt ligands and Pb^{2+}-rich nanocrystal surfaces [5, 9, 10]. In this study, we further improve on this strategy and apply newly designed polysalt ligands for the stabilization of green-emitting nanocubes (NCs) and blue emitting $CsPbBr_3$ nanoplatelets (NPLs). In particular, we show that our polysalt ligands can be applied as prepared to stabilize and passivate $CsPbBr_3$ NCs with great effectiveness. However, stabilization of the NPLs could not be achieved using the as-synthesized polymer. Instead, we found that premixing the polymer with bromide-based salts (to form polysalt-complexes) can simultaneously promote structural integrity, enhance the PL properties and improve the colloidal stability of the NPLs.

Materials and methods

$CsPbBr_3$ nanocrystal growth

The growth of $CsPbBr_3$ NCs was performed using the hot injection method developed by Kovalenko et al. [2]. Briefly, two precursor solutions were prepared. First, a cesium solution was prepared by dissolving Cs_2CO_3 and oleic acid in octadecene (ODE) at 120 °C. Second, a Pb-bromide solution was prepared by mixing $PbBr_2$ with equimolar amounts of OA and OLA in ODE and letting the mixture stir at 120 °C until the solution became clear. Then, the Cs-oleate precursor solution was injected into the Pb-bromide solution at

✉ Hedi Mattoussi
mattoussi@chem.fsu.edu

[1] Department of Chemistry and Biochemistry, Florida State University, Tallahassee, FL 32306, USA

Published online: 06 April 2023

160 °C to promote the growth of $CsPbBr_3$ nanocrystals. Further details on the employed synthetic steps and purification are provided in reference [11].

$CsPbBr_3$ nanoplatelet growth

The NPLs used in this study were grown under room temperature following the method introduced by Bohn et al., but adjustments were implemented to accommodate a larger scale reaction [12, 13]. A Cs-oleate precursor solution was prepared by heating at 80 °C a mixture of Cs_2CO_3 (0.1 mmol, 32.6 mg) and OA (10 mL) until the content became clear. Similarly, a $PbBr_2$ solution was prepared by dissolving $PbBr_2$ (0.5 mmol, 183.5 mg) in a mixture of OA (500 µL), OLA (500 µL) and toluene (50 mL), then continuously stirred it at 80 °C until dissolution of the salt (~ 2 h). Growth of NPLs was carried by adding the Cs-oleate precursor (500 µL) to the $PbBr_2$ precursor (5 mL), which yielded a yellowish solution. After ~ 1 min 6 mL of acetone was rapidly added. The solution was initially clear, then gradually became turbid. After 5 min of stirring, the mixture was centrifuged at 3600 RPM for 10 min, the supernatant was discarded, and the precipitate was re-dispersed in 4 mL of hexane and stored for further use [12].

Ligand synthesis

We used one representative set of polysalt ligands in which each macromolecule presents ~ 8 imidazolium bromide (IMB) salt groups and ~ 32 octadecylamine (ODA) solubilizing alkyl motifs. The polysalt synthesis relied on the nucleophilic addition reaction between a low molecular weight poly(isobutylene-alt-maleic anhydride) (PIMA, MW 6000 Da, ~ 39 to 40 monomers) and a mixture of amine-imidazole along with ODA nucleophiles. Briefly, PIMA (1 g, 6.64 mmol monomer) was dissolved in DMF (5 mL). Then, 1-(3-aminopropyl) imidazole (158.71 µL, 1.33 mmol) dissolved in 5 mL DMF was added to the PIMA solution while stirring at 60 °C. After approx. 30 min, ODA (1.44 g, 5.33 mmol) dissolved in chloroform under moderate heat was added and the reaction was stirred overnight. After evaporating the solvent, column chromatography was employed to purify the product using chloroform as the eluting solvent, yielding a single fraction containing the desired product [11]. The isolated product was dried using a rotary evaporator, then subjected to an alkylation reaction to introduce quaternary amine groups on the imidazole in addition to bromide ions. This was done by transferring the intermediate product to a pressure vial and dissolving it in 10 mL THF. Excess bromoethane (5 mL) was added and the solution was left to react overnight under reflux conditions (~ 70 °C). After evaporating the solvent, the product was then washed several times with ethyl acetate and dried in a vacuum oven at 50 °C for a few hours to obtain the final product as a white powder.

Ligand exchange

First, polysalt ligand (15 mg) was added to toluene (400 µL) and the mixture was left stirring until complete dissolution. This solution was mixed with stock solution of $CsPbBr_3$ NC in hexane (200 µL) and the mixture sonicated for ~ 5 min. The content was washed once with excess ethanol and centrifuged (3500 RPM, 5 min). The supernatant containing the native ligands was discarded and the remaining NCs were redispersed in toluene (400 µL).

Ligand exchange of the NPLs with the polysalt/$PbBr_2$ complex was implemented in two steps. Firstly, polysalt-$PbBr_2$ complex was prepared by combining the IMB-polymer (40 mg, 0.02 mmol anchoring groups) and $PbBr_2$ (5 mg, 0.0136 mmol) in a 10-mL vial containing 2 mL of toluene. After stirring at 60 °C until complete dissolution, the mixture was allowed to cool and then centrifuged at 3500 RPM for 5 min. The precipitate was discarded and the supernatant containing the complex was stored until further use. Preparation of the polysalt-$CoBr_2$ complex followed a similar process to the one described for polysalt-$PbBr_2$ complex. In the second step, ligand exchange of the NPLs was implemented by adding 400 mL of the polysalt-complex solution to the NPL dispersion (200 µL) in a 10-mL scintillation vial. After sonication for ~ 1 to 2 min the mixture was washed one time with excess ethyl acetate and centrifuged (4000 RPM, 5 min). The supernatant was discarded and the NPLs were redispersed in toluene (400 µL).

Optical characterization

Absorption spectra were collected using a UV–vis absorption spectrophotometer (UV 2450 model, Shimadzu, Columbia, MD). Fluorescence spectra were collected using a Fluorolog-3 spectrofluorometer (HORIBA Jobin Yvon, Edison, NJ) equipped with a TBX PMT detector and the excitation wavelength was set at 350 nm. Time-resolved PL lifetimes were obtained using a time correlation single photon counting (TCSPC) setup integrated within spectrofluorometer. NanoLED-440LH (100 ps, FWHM) provided a pulsed laser at 440 nm with a repetition rate at 1 MHz. The time-resolved profiles were fit using a triexponential decay function:

$$I(t) = \alpha_1 e^{-\frac{t}{\tau_1}} + \alpha_2 e^{-\frac{t}{\tau_2}} + \alpha_3 e^{-\frac{t}{\tau_3}}, \quad (1)$$

here t is time and α_i is a weighted parameter corresponding to each decay time, τ_i. To extract an average amplitude-weighted lifetime, τ, the following expression was used:

$$\tau = \frac{\sum \alpha_i \tau_i^2}{\sum \alpha_i \tau_i} \quad (2)$$

Absolute PLQY measurements were obtained with a Hamamatsu Quantaurus absolute PL quantum yield spectrometer (Bridgewater, NJ) equipped with an integrating sphere (C11347). The samples were prepared with an optical density of ~ 0.1 at $\lambda_{exc} = 400$ nm.

Structural characterization

Powder X-ray diffraction (PXRD) patterns were collected with a Rigaku MiniFlex 6G, equipped with a Cu-Kα source ($\lambda = 1.5406$ Å) and D/TeX Ultra 2 silicon strip detector. The instrument was operated at 15 mA and 40 kV with a scan rate of 5°/min over a 2θ range from 10° to 60° with a step-size of 0.01°. Sample preparation was done by drop-casting concentrated dispersions of each nanocrystal sample onto a silicon sample holder (10 mm diameter, 0.2 mm deep well) and allowing it to dry under nitrogen flow.

Results and discussion

Growth of $CsPbX_3$ (X = Cl, Br, or I) perovskite quantum dots (PQDs) yields materials that are surface capped with a mixture of OA and OLA ligands, which are classified as hard Lewis acid and Lewis base, respectively [8]. They exhibit rather weak coordination interactions with the NC surfaces. This results in high rates of desorption, which destabilizes the nanocrystal surfaces. Degradation of the as-prepared perovskite NCs can be caused by environmental conditions during storage, or post-synthesis processing, like washing with polar solvents. These tend to cause ligand detachment which negatively affect the integrity of the PQDs. Deterioration of the nanocrystals alters the stoichiometry of the anion-rich NC surfaces, yielding Pb^{2+}-rich sites combined with Cs^+ and Br^- vacancies that act as trap states within the bandgap of the material [7]. The photophysical properties of semiconductors are known to be strongly affected by surface defects, particularly for nanoscale materials due to their high surface-volume ratios [14]. Consequently, the measured PL intensities for these materials are lower than what these perovskites can offer. Thus, repairing the surface defects is critical to obtaining high quality nanocrystals with optimized photophysical properties. A few literature studies have reported that defective $CsPbX_3$ nanocrystal surfaces can be restored using salt-containing molecules, such as didodecyl dimethyl ammonium bromide (DDAB) [5, 9, 10]. These molecules act as vacancy fillers and surface stabilizers of the $CsPbBr_3$ QDs, where the ammonium cations fill the Cs^+ vacancies while free Br^- anions bind to under-coordinated Pb^{2+} sites. This reduces the density of trap states, yielding materials that exhibit high PL and improved structural integrity. Although promising, small molecule ligands still exhibit dynamic binding and impart poor steric stabilization. This tends to yield materials with limited long-term colloidal and photophysical stability.

Here, we have tested the ability of a multi-coordinating polysalt ligand to provide a few key benefits: (1) promoting strong binding interactions onto the PQD surfaces, (2) repairing the surface defects, (3) removing surface traps which enhances the PL properties of the PQDs, and (4) imparting long term colloidal stability. Synthesis of the polysalt ligand relies on the high reactivity of succinic anhydride rings (along the PIMA chain) with amine-nucleophiles, via the nucleophilic addition reaction. Figure 1b schematically summarizes the reaction steps employed for preparing a polymer that contains several IMB groups and multiple ODA. In this structure, the salts serve as anchoring groups, while the alkyl chains promote affinity to organic solvents and impart steric stability to the nanocrystals. Using the conditions described, we prepared a polysalt that has ~ 8 IMB groups and ~ 32 ODA chains. The ligand stoichiometry was confirmed by ^{1}H NMR spectroscopy as shown in Fig. 1c.

In the first series of experiments, we performed ligand exchange onto green-emitting $CsPbBr_3$ nanocubes. We measured a substantial improvement in the PL properties as well as improved structural and colloidal stability following substitution of the native OLA/OA ligands with the polysalt. By matching the optical densities of the first exciton peak in the absorption profiles for all the new ligand-coated nanocrystals with their respective native OLA/OA-coated counterparts, we were able to quantify the PL enhancement by comparing the intensity values at the peak wavelength (i.e., at ~ 500 nm for NCs, see Fig. 2a). The nearly identical absorption spectra of the NCs suggests that the nanocrystal integrity is not altered after ligand exchange. The polysalt-coated NCs showed approx. 1.6 times greater PL intensity than that of the native sample. The absolute PLQY of the NCs increased after ligand substitution from 65% to near unity at 95% (Fig. 2d). We also evaluated the integrity of the nanocubes during ligand substitution by acquiring powder diffraction from the sample before and after ligand substitution. The XRD patterns acquired for both samples were compared to the standard orthorhombic bulk $CsPbBr_3$ XRD (ICSD 243735). The XRD patterns shown in Fig. 4a, reveal that the crystal structures of the as-grown (OLA/OA-stabilized) sample and the polysalt-stabilized one are essentially identical. Furthermore, the structure is consistent with *Pnma* orthorhombic crystal structure measured form bulk perovskite samples.

However, when applying the as-synthesized polysalt ligands to blue-emitting NPLs, we observed a drastically different behavior. More precisely, upon mixing the NPLs

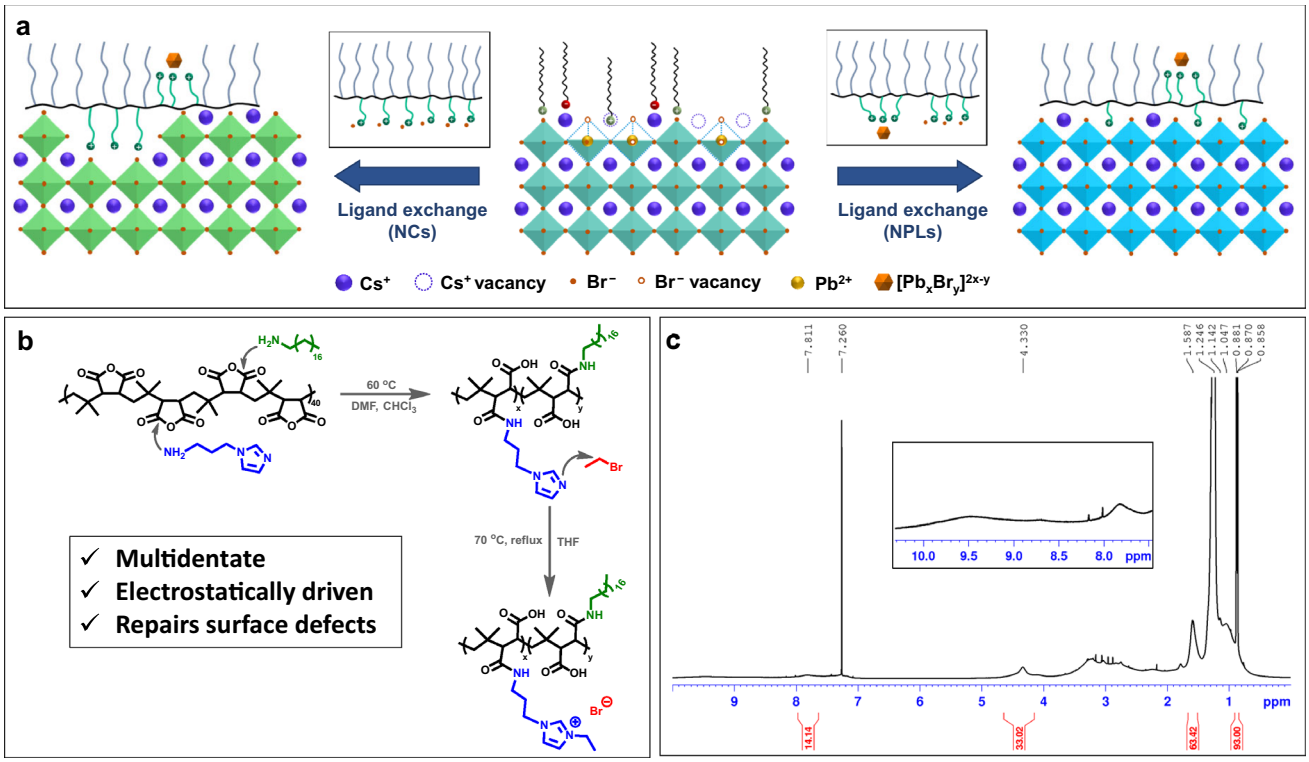

Fig. 1 **a** Schematic representation of Cs^+ and Br^- vacancy passivation using polysalt ligand on NCs (left) and polysalt/$PbBr_2$ ligand on NPLs (right); formation of high-valence lead bromide complexes via etching or from ligand complexation is depicted. **b** Nucleophilic addition and quaternization reaction of IMB-based ligand synthesis. **c** ^1H NMR spectrum of IMB (i.e., IMB-PIMA-ODA polymer) ligand in $CDCl_3$

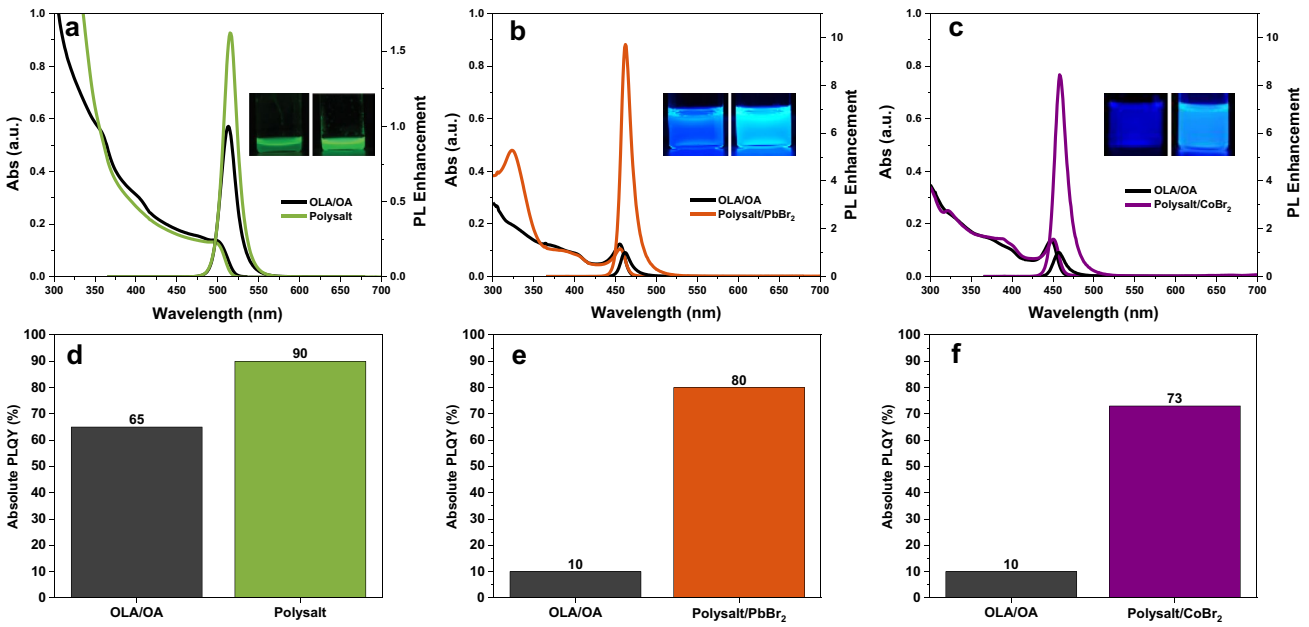

Fig. 2 **a** Absorption and emission profiles along with fluorescence images of native (left) and polysalt ligand-coated NCs (right). **b** Absorption and emission profiles of OLA/OA- and polysalt/$PbBr_2$-coated NPLs. **c** Absorption and emission profiles with fluorescence images of native and polysalt/$CoBr_2$-coated NPLs. **d** Absolute PLQYs of samples in **a**. **e** Absolute PLQYs of samples in **b**. **f** Absolute PLQYs of samples in **c**

with a solution of the ligands a pronounced increase in the PL signal was measured, but that increase was coupled with a decrease in the nanoplatelet concentration. The decrease in concentration was found to be more pronounced when higher amounts of the polymer were introduced (see Fig. 3). If the mixture is tracked for several days of storage time, the NPL dispersions consistently exhibited a sizable decay in the PL intensity which can be accompanied by a slow shift in the PL profile from blue to green, indicating that the NPL morphology has also changed to nanocubes [12]. In addition to the decrease in PL intensity, the absorbance profile developed a new pronounced feature at 320–325 nm which increases with the amount of polysalt ligand added. Literature data indicate that this feature is associated with the formation of a $[Pb_xBr_y]^{2x-y}$ complex [12]. Thus, the data shown in Fig. 3 can be attributed to etching of the nanoplatelets upon interactions with the introduced polymer. Here, free bromide ions from the ligand extract surface Pb^{2+} to form these high-valence complexes and hence cause a significant fraction of the NPLs to progressively disintegrate with time. The deleterious effects of the polysalt on the integrity of the NPLs (in comparison to NCs) can be ascribed to the rather high surface energy of the anisotropic NPLs, which produces faster etching of the larger longitudinal surface area, producing smaller concentration of NPLs combined with the buildup of higher valence $[Pb_xBr_y]^{2x-y}$ complexes.

Having gained an understanding of the subtle effects of the ligand strong interaction with the NPLs, we then reasoned that promoting the formation of such salt complexes ($[Pb_xBr_y]^{2x-y}$) by mixing the polymer with $PbBr_2$ salt prior to mixing with the NPLs would be beneficial (Fig. 1a). This rationale is similar to the approach used by Kovalenko et al. who pre-complexed the DDAB ligand with $PbBr_2$ to better repair surface damages of perovskite NCs [9]. Additionally, this compound may have the ability to restore damaged $PbBr_6$ octahedra within the nanocrystals and maintain the overall structural integrity. And indeed, we found that premixing the polymer with $PbBr_2$ salt constituting a molar ratio of ligand anchors to $PbBr_2$ of ~ 1:0.7 has yielded the best results in terms of achieving the highest PL enhancement coupled with preserved NPL morphology and structural integrity. Our data also showed that using lower molar ratio than the above value (~ 1:0.7) produces PL enhancement that is coupled with digestion of defective NPLs in the medium.

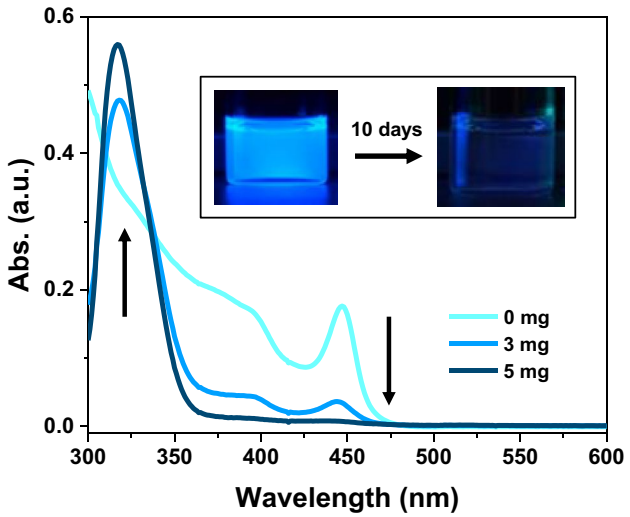

Fig. 3 Addition of different amounts of polysalt ligand (in mg) yields a decrease in absorption at the first exciton peak (450 nm) paired with an increase in absorption of a new peak (325 nm) that corresponds to formation of $[Pb_xBr_y]^{2x-y}$ complex due to etching. Images show loss of nanocrystal concentration of polysalt-coated NPLs after 10 days of storage

The absorption spectra of the NPLs for both ligand-salt complex-coated NPLs indicate the preservation of nanocrystal integrity after applying the new ligands. The PL profile of polysalt/$PbBr_2$-coated NPLs show an intensity of almost 10 times greater compared to the as-grown NPLs.

For blue-emitting NPLs, it is crucial to ensure color purity by maintaining a narrow emission band at ~ 460 nm (see Fig. 2b, e). Upon introduction of the polysalt/$PbBr_2$, we observe no shift in the PL spectrum and the FWHM remains ~ 16 nm (Fig. 2b). The preserved absorption and PL profiles indicate that the NPLs with the new ligand/salt complex exhibit strong quantum confinement of charge carriers and consistently preserve a three-monolayer structure [13, 15, 16]. Additionally, the XRD patterns collected from NPLs indicates that the orthorhombic perovskite phase is retained after the ligand exchange process with the polysalt/$PbBr_2$ complex (Fig. 4b).

Having achieved both higher PL and preserved integrity of the nanocrystals, we reasoned that other metal-bromide salts can likewise be used in place of $PbBr_2$ [17]. Cobalt has properties similar to that of lead, specifically the comparable sizes of their ionic radii, which suggest that it may be a promising candidate to explore. Therefore, we chose to examine the system further by premixing $CoBr_2$ with the ligand and observing its effects on the optoelectronic properties of the NPLs. The data shown in Fig. 2c, f prove that pre-reacting $CoBr_2$ with the polysalt followed by mixing with NPLs produce unchanged absorption and PL profiles that are comparable to freshly prepared dispersions. Furthermore, a PL enhancement of ~ 8 was measured compared to the as-grown NPLs. The PLQY values measured for NPLs stabilized with both the polysalt-complexes (Pb or Co-based) are considerably higher than their native counterparts, increasing from 10 to 70–80% (Fig. 2b, c, e, f). We are presently investigating the utility of other Br-based salts (e.g., $NiBr_2$ and $ZnBr_2$) to evaluate whether pronounced levels of PL enhancements are measured while preserving the absorption and PL profiles.

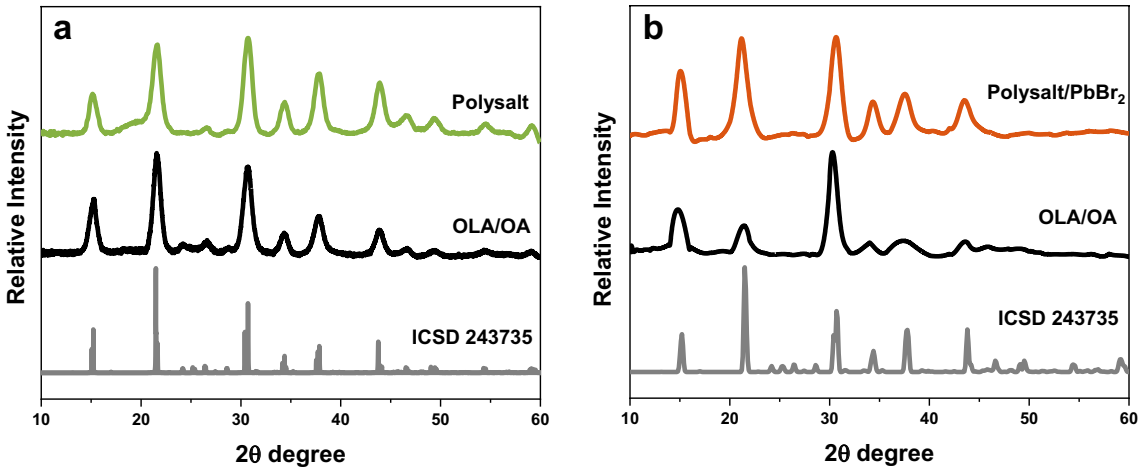

Fig. 4 **a** Powder XRD patterns of OLA/OA- and polysalt-coated NCs together with standard bulk $CsPbBr_3$. **b** Powder XRD patterns collected from native ligand- and polysalt/$PbBr_2$-coated NPLs

We are also looking into identifying whether or not the formation of transition metal-bromide salt complexes with higher valences plays important in the passivation of the NPLs. We hope to report on those findings in the future.

Conclusion

In this study, we reported on the ability of a polysalt ligand that combines imidazolium bromide salt motifs along a polymer backbone to strongly coordinate onto $CsPbBr_3$ perovskite nanocrystals. In particular, we found that when applied to $CsPbBr_3$ NPLs, they trigger surface defect removal while promoting long term structural and colloidal stability. The optical data confirm that bromide-based salt ligands are efficient at filling Cs^+ and Br^- vacancies and passivating Pb^{2+} sites, resulting in increased PLQY. Additionally, while etching is prevalent in both species of nanocrystals investigated, the data provided demonstrates that the effects are negligible for NCs. Reducing these effects of surface etching in NPLs involved the addition of a bromide-based salt to the polysalt ligand, which successfully prevented the deterioration of the nanocrystal structure and photophysical properties.

Acknowledgments The authors thank FSU and the National Science Foundation (NSF-CHE #2005079), and Kasei-Asahi for financial support.

Declarations

Competing interests The authors declare no competing financial interest.

References

1. J. Shamsi et al., Metal halide perovskite nanocrystals: synthesis, post-synthesis modifications, and their optical properties. Chem. Rev. **119**, 3296–3348 (2019)
2. L. Protesescu et al., Nanocrystals of cesium lead halide perovskites ($CsPbX_3$, X = Cl, Br, and I): novel optoelectronic materials showing bright emission with wide color gamut. Nano Lett. **15**, 3692–3696 (2015)
3. E.M. Sanehira et al., Enhanced mobility $CsPbI_3$ quantum dot arrays for record-efficiency, high-voltage photovoltaic cells. Sci. Adv. **3**, eaao4204 (2017)
4. T. Chiba, J. Kido, Lead halide perovskite quantum dots for light-emitting devices. J. Mater. Chem. C **6**, 11868–11877 (2018)
5. J. Pan et al., Highly efficient perovskite-quantum-dot light-emitting diodes by surface engineering. Adv. Mater. **28**, 8718–8725 (2016)
6. J. De Roo et al., Highly dynamic ligand binding and light absorption coefficient of cesium lead bromide perovskite nanocrystals. ACS Nano **10**, 2071–2081 (2016)
7. M.I. Bodnarchuk et al., Rationalizing and controlling the surface structure and electronic passivation of cesium lead halide nanocrystals. ACS Energy Lett. **4**, 63–74 (2019)
8. R.L.Z. Hoye et al., Identifying and reducing interfacial losses to enhance color-pure electroluminescence in blue-emitting perovskite nanoplatelet light-emitting diodes. ACS Energy Lett. **4**, 1181–1188 (2019)
9. M. Imran et al., Simultaneous cationic and anionic ligand exchange for colloidally stable $CsPbBr_3$ nanocrystals. ACS Energy Lett. **4**, 819–824 (2019)
10. Y. Shynkarenko et al., Direct synthesis of quaternary alkylammonium-capped perovskite nanocrystals for efficient blue and green light-emitting diodes. ACS Energy Lett. **4**, 2703–2711 (2019)
11. S. Wang et al., Polysalt ligands achieve higher quantum yield and improved colloidal stability for $CsPbBr_3$ quantum dots. Nanoscale **13**, 16705–16718 (2021)
12. S. Wang et al., Engineering highly fluorescent and colloidally stable blue-emitting $CsPbBr_3$ nanoplatelets using polysalt/$PbBr_2$ ligands. Chem. Mater. **34**, 4924–4936 (2022)

13. B.J. Bohn et al., Boosting tunable blue luminescence of halide perovskite nanoplatelets through postsynthetic surface trap repair. Nano Lett. **18**, 5231–5238 (2018)
14. M.A. Boles et al., The surface science of nanocrystals. Nat. Mater. **15**, 141–153 (2016)
15. Q.A. Akkerman et al., Solution synthesis approach to colloidal cesium lead halide perovskite nanoplatelets with monolayer-level thickness control. J. Am. Chem. Soc. **138**, 1010–1016 (2016)
16. C. Otero-Martínez et al., Colloidal metal-halide perovskite nanoplatelets: thickness-controlled synthesis, properties, and application in light-emitting diodes. Adv. Mater. **34**, 2107105 (2022)
17. X. Zhang et al., Stable blue-emitting $CsPbBr_3$ nanoplatelets for lighting and display applications. ACS Appl. Nano Mater. **5**, 17012–17021 (2022)